Int. J. Electrochem. Sci., 15**(2020)** 11180 – 11190, doi: 10.20964/2020.11.58

International Journal of
ELECTROCHEMICAL
SCIENCE
www.electrochemsci.org

Effect of Composite Additives on the Zinc Anode of Zinc–Nickel Single-Flow Batteries

Shouguang Yao[1,*], *Dapei Ding*[1,2], *Jie Cheng*[2,3], *Hao Xu*[1,3], *Yusheng Yang*[2,3]

[1]School of Energy and Power Engineering, Jiangsu University of Science and Technology, Zhenjiang, Jiangsu 212003, China
[2]ZhangjiagangSmartgridFanghua electrical energy storage research institute Co., Ltd., Zhangjiagang 215600, China
[3]Chilwee Power Co., Ltd., Huzhou 313100, China
[*]E-mail: zjyaosg@126.com

Received: 3 May 2020/ *Accepted:* 13 June 2020 / *Published:* 30 September 2020

In this study, a nickel-plated steel strip was used as the base material of zinc electrodes. The effect of composite additives, such as Sn^{4+}, Ga^{3+},and Pb^{2+}, on zinc deposition and dissolution was tested using cyclic voltammetry, SEM, and constant-current charge/discharge. The cyclic voltammetry results showed that the composite additives could codeposit with zinc and easily form uniform crystal nuclei and dense deposit layers. The Tafel polarization curves demonstrated that the hydrogen evolution reaction on the electrodes in the solution with composite additives was weaker than those of the base solution and a single additive. The constant-current charge/discharge results presented that electrodes in the solution with composite additives obtained high coulombic efficiency but not significantly higher than that of the base solution and a single additive. The SEM results showed the smooth zinc deposit morphology with composite additives and small zinc deposit particles. The results of the self-discharge test demonstrated that the self-discharge performance of the base solution clearly improved with the addition of composite additives and the residual capacity increased from 49.7% to 65.6% after 24 h in standby state.

Keywords: Zinc–nickel single-flow battery; Composite additives; Charge retention; Coulombic efficiency

1. INTRODUCTION

Zinc electrodes demonstrate excellent performance due to their characteristics of rich resources, low equilibrium potential, good reversibility, and environmental safety. Hence, these electrodes are widely used in chemical power sources, especially alkaline zinc series batteries[1–3]. However, zinc electrodes can cause fading in the battery capacity and cycle performance due to their disadvantages, such as dendrites, passivation, corrosion, electrode deformation, and severe self-discharge during the

charge/discharge process[4]. At present, researchers usually improve the electrochemical performance of zinc electrodes by mixing additives and changing the electrolyte composition. Yang's group[5] determined that the use of foamed brass as the current collector of zinc electrodes could improve the charge/discharge performance of zinc electrodes and suppress the growth of zinc dendrites. Liu's group[6] discovered that the lead plating on the surface of traditional negative-electrode current collectors effectively reduced the hydrogen evolution of negative electrodes. The current density of hydrogen evolution on the surface of the current collector was below 1.0 mA/cm^2 under the open-circuit potential. Liu's group[7] used N,N,N-trimethyl-1-dodecanaminium bromide （DTAB） to inhibit the passivation and corrosion of zinc electrodes and alleviate the growth of zinc dendrites, but the problems of zinc electrodes still persist.

The problem of zinc dendrites is solved by using zinc–nickel single-flow batteries with flowing electrolyte and controlled zinc deposition and dissolution. The electrolyte containing zinc oxide can stabilize the structure of nickel hydroxide and remarkably improve the overall cycle performance of the battery[8,9]. However, problems, such as continuous hydrogen evolution and serious self-discharge of the zinc anode, still exist[10]. At present, the electrochemical performance of zinc electrodes in zinc–nickel single-flow batteries was improved by changing the anode substrate and optimizing the electrolyte composition. Wen' group[11]investigated the additives in zinc deposition and dissolution by adding lead and tungstate ions to the alkaline zincate solution. They found that these two additives could produce additional uniform and dense deposits, reduce the growth of sponge zinc, and improve the charge/discharge performance of the battery. Wang's group[12] explored the effect of Bi^{3+} and tetrabutylammonium bromide(TBAB) on the dendrite growth behavior of zinc electrodes in alkaline zincate solutions. The experimental results showed that Bi^{3+} and TBAB could inhibit the dendrite growth of zinc electrodes to some extent, but TBAB failed to inhibit the dendrite growth effectively under high cathodic overpotential. Chen's group[13] added potassium stannate to the potassium zincate solution to improve the deposition morphology and self-discharge performance of zinc anodes.

On the basis of previous investigations, this study aimed to explore the effect of composite additives, including Sn, Ga, and Pb ions, on zinc deposition and dissolution. Electrochemical testing methods, such as cyclic voltammetry, constant-current charge/discharge, and SEM surface analysis, were used to examine the effect of different additives on the zinc deposition behavior, ensure the selection of appropriate additives, and improve the battery performance.

2. EXPERIMENTAL SECTION

2.1 Configuration of electrolyte

The chemical reagents used in this experiment were all analytically pure. KOH was purchased from Tianjin Bodi Chemical Co., Ltd. (China). LiOH and ZnO were obtained from Jiangsu Qiangsheng Functional Chemistry Co., Ltd. (China). The basic solution, denoted solution A, was composed of KOH (8 mol/L), LiOH (5 g/L), and ZnO (0.5 mol/L). Various solutions containing Sn, Ga, or Pb ions were prepared by adding different qualities of potassium stannate, metal gallium, or

lead oxide to solution A, respectively. These resultant solutions were denoted as B (A+0.05 mol/L Sn^{4+}), C (A+0.05 mol/L Ga^{3+}), D (A+0.05 mol/L Sn^{4+}+0.05 mol/L Ga^{3+}), E (A+0.05 mol/L Sn^{4+}+0.05 mol/L Ga^{3+}+0.0001 mol/L Pb^{2+}), and F (A+0.05 mol/L Sn^{4+}+0.05 mol/L Ga^{3+}+0.001 mol/L Pb^{2+}).

2.2 Pretreatment of negative current collector and preservation of sample

Since nickel-plated steel strips can change the mass transfer manner, improve the deposition efficiency and reduce the side hydrogen evolution reaction[14], a nickel-plated steel strip was used as the current collector of the negative electrode in the experiment. Before the experiment, the negative electrode was degreased with ethanol and placed in 10% dilute sulfuric acid for 1 min to remove the surface oxide film. Then, the electrode was washed with deionized water and immediately placed in an aqueous solution of sodium hypophosphite (10 wt%) for later use. Before the negative electrode test, the electrode was rinsed with deionized water. To ensure that both sides of the surface area of the negative electrode substrate are in contact with the electrolyte, the pole ears were wrapped with polytetrafluoroethylene tape before the experiment.

2.3 Performance test

The tests were conducted at room temperature with magnetic stirring. The working electrode size was 1 cm×1 cm. The 2 cm×2 cm sintered nickel electrode was used as the counter electrode on both sides of the working electrode. The reference Hg/HgO and first two electrodes formed a three-electrode system. The electrolyte was the aforementioned solution. Cyclic voltammetry test, SEM analysis sample preparation, electrochemical impedance spectroscopy (EIS), Tafel polarization test, and constant-current charge/discharge test were performed using the CHI608E electrochemical station (Shanghai Chenhua Instrumental Co., Ltd.; China). The sweep speed and voltage range of the cyclic voltammetry test were1 mV/s and −0.6 to −1.6 V, respectively[14]. Multiple scans were performed until the curves coincided. By charging the scanning electron microscopy (SEM) samples with a current density of 20 mA/cm^2 for 500 s, their coatings were obtained, and then washed and stored. A scanning electron microscope (2502M, K23,UK) was used to analyze the SEM surface morphology. The EIS evaluation was conducted in the test frequency range and disturbance amplitude of 0.01 Hz–100 KHz and 5 mV, respectively. The scanning voltage range and scanning speed of the Tafel polarization test were −0.6 to −1.6 V and 1 mV/s, respectively. In the constant-current charging/discharging test, the working electrode was charged at a current density of 40 mA/cm^2 for 7200 s and then discharged at the same current density to −0.6 V.

The self-discharge performance of the zinc–nickel single-flow battery was characterized by the capacity retention rate after the battery was left to stand for a certain period of time[13]. The method is described as follows. The size of the negative electrode was 2 cm×2 cm, and the 2 cm×2 sintered nickel electrode was used as the counter electrode on both sides of the negative electrode to ensure that a two-electrode system was formed. The self-discharge test was then carried out using a CT2001A tester (Jinnuo Wuhan Corp., China). The sintered nickel electrode must be activated before

testing[8]. The battery was charged with a constant current of 20 mA/cm^2 to a cutoff of 160 mA·h and then allowed to stand for 24 h. The solution continuously flowed while standing, and the battery was finally discharged with a constant current of 20 mA/cm^2 to 1.2 V.

3. RESULTS AND DISCUSSION

3.1 Analysis of cyclic voltammetric curves

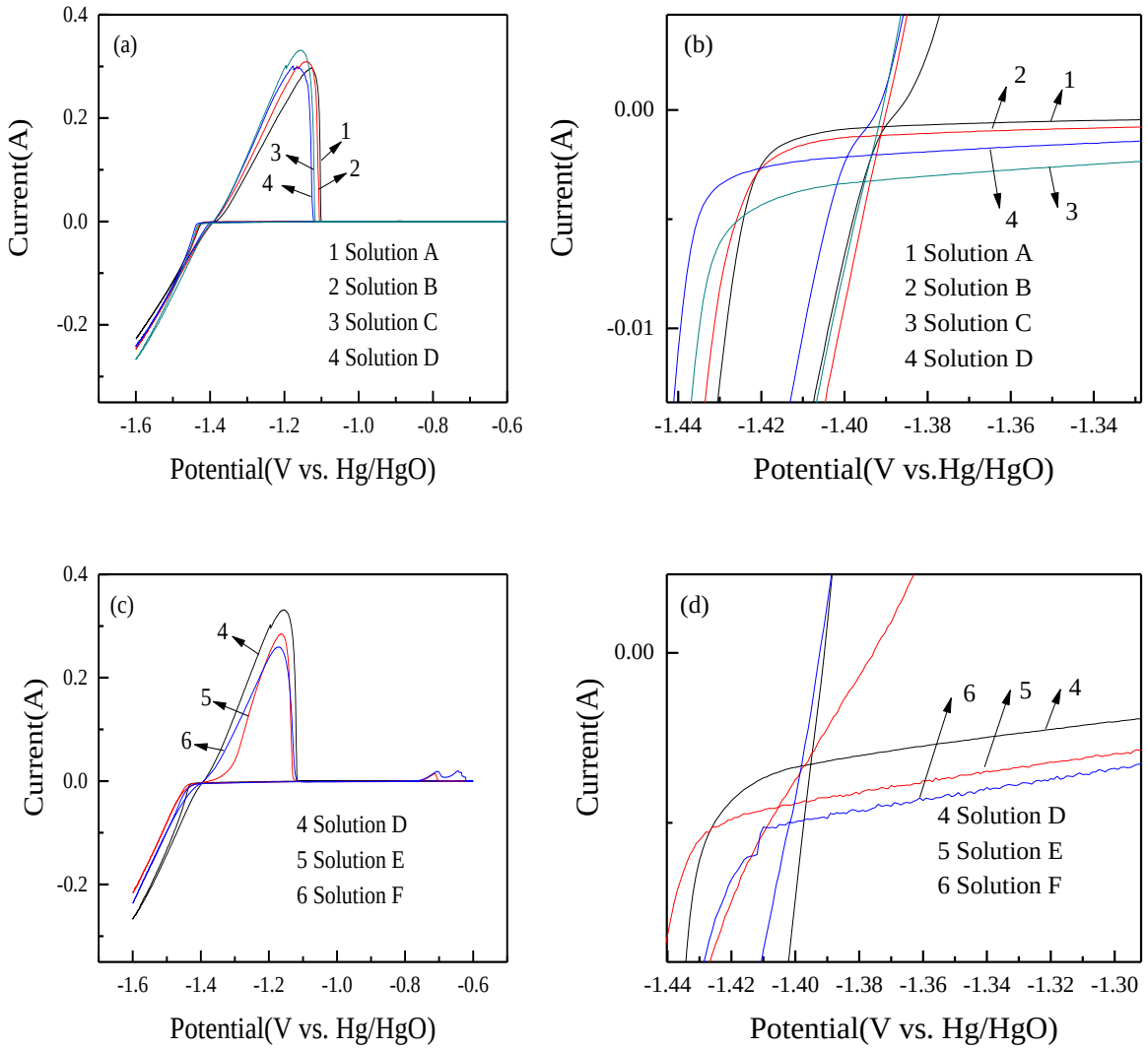

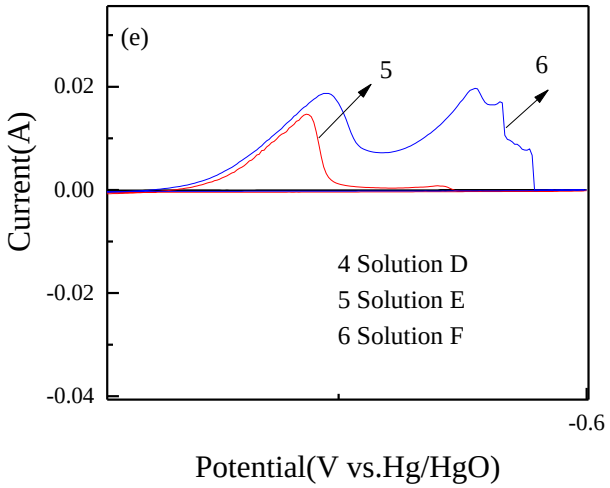

Figure 1. Cyclic voltammetric curves of different solutionsat a scan rate of 1 mV/s: (a)(b)solutions A, B, C, and D; (c)(d)(e)solutions D, E, and F

Figure 1 illustrates the cyclic voltammetric curves of 1 mV/s obtained from the nickel-plated steel strip electrodes in different solutions. Figure 1(a) presents the cyclic voltammetric curves of solutions A, B, C, and D, Figure 1(b) is a partial enlargement of Figure 1 (a). When the first negative scan reached approximately−1.45 V, the sharp increase in the current response of the electrode in the four solutions indicated that significant zinc deposition occurred. The appearances were caused by the crystal seed formation and crystal plane growth when the potential was sufficiently negative[15]. When the potential was reversely scanned from −1.6 V, zinc deposition on the electrode continuously occurred and the deposition current continuously decreased. The anode peaks of the electrode in the four solutions appeared around −1.18 V, and the anode peak current values occurred in the order of solutions D, C, B, and A from large to small. The very low anode peak around −0.89 V that only appeared in solutions A and B may be caused by the oxidation of zinc–nickel alloys[14]. A stable alloy group may have been formed after adding Ga. As shown in Figure 1(b), compared with solution A, the gradual deviation in the cathode branch of the cyclic voltammetry curve with Sn or Ga added in the solution from the zero current line at around −1.17 V is likely caused by the codeposition of Sn, Ga, and zinc[16]. Figure 1(c) illustrates the cyclic voltammetry curves of the electrode in solutions D, E, and F, Figure 1(d) and Figure 1(f) are partial enlargements of Figure 1 (c). Apart from the anode peak at around −1.18 V, the two anode peaks appearing between −0.6 and −0.8 V in solutions E and F(see Figure 1(e)) are likely related to the dissolution of Pb[17]. This finding indicated that Pb and Zn codeposition may occur. Figure 1(d) demonstrates that the cathode branch of the cyclic voltammetry curve from the zero current line gradually deviated with the increase in Pb concentration. This finding was likely due to the codeposition of Sn, Ga, and Pb with zinc.

Nucleation overpotential (NOP) indicates the extent of polarization of a cathode and is defined as the difference between equilibrium potential (E_{equ}) and deposition potential (E_{dep})[18]. According to the cyclic voltammetry curve in Figure 1, the NOP values of different solutions are summarized in Table 1[18,19]. Table 1 shows that solutions A and F have the lowest and highest E_{equ} and E_{dep} values, respectively. The additives reduced E_{equ} and E_{dep}[13], easily generated uniform crystal

nuclei, and formed a dense deposition layer[18,19]. Among the six solutions, the largest NOP value of solution D indicated that solution D had strong cathodic polarization. The smaller NOP values of solutions E and F than that of solution D indicated that Pb could inhibit cathodic polarization likely due to the interaction between composite additives.

Table 1. Equilibrium potential, deposition potential, and NOP values of the electrode in different solutions

	E_{equ}/V	E_{dep}/V	−NOP/mV
A	−1.390	−1.422	32
B	−1.391	−1.427	36
C	−1.399	−1.435	36
D	−1.395	−1.439	44
E	−1.401	−1.439	38
F	−1.402	−1.441	39

3.2 Analysis of polarization curves

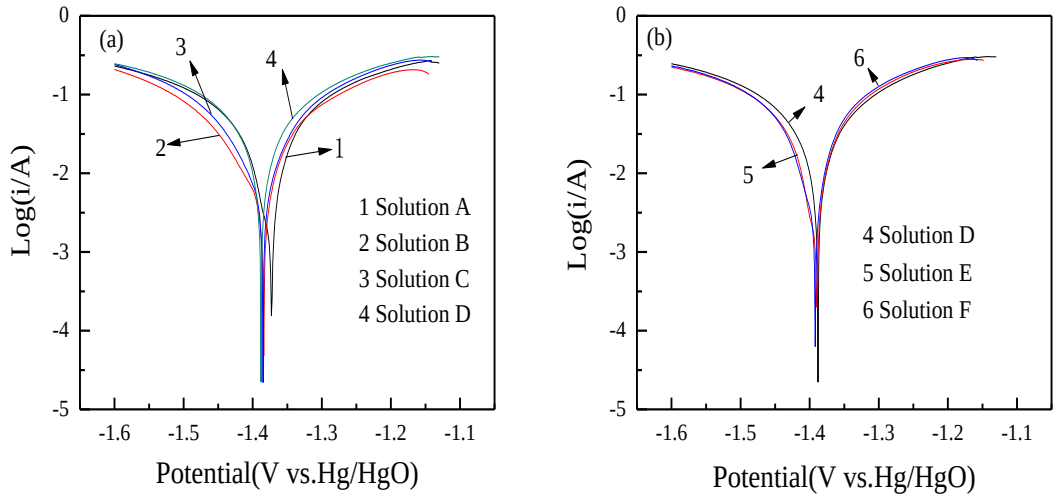

Figure 2. Tafel polarization curves of different solutions: (a)solutions A, B, C, and D; (b)solutions D, E, and F

Table 2. Kinetic data of zinc deposition and dissolution in different solutions

	E_0(V)	$I_0(mA/cm^2)$	B_a(mV/dec)	B_c(mV/dec)
A	−1.373	3.334	97.	65
B	−1.384	3.346	88	78
C	−1.385	3.364	77	73
D	−1.388	3.394	54	54
E	−1.390	3.350	96	63
F	−1.392	3.256	76	61

We performed 10 charge-discharge cycles on the 6 solutions, then electroplated at a current density of 10 mA/cm^2 for 300s to obtain a Tafel curve. Finally, we used CorrView2 software to fit the Tafel curve to obtain kinetic data of zinc deposition and dissolution. Figure 2 illustrates the Tafel polarization curve and Table 2 lists the anode and cathode Tafel slope (B_a and B_c), formal potential (E_0), and exchange current density (I_0) values. Inhibition of hydrogen evolution is a key factor in the zinc deposition process. The rate of hydrogen evolution reaction depends on the overpotential of hydrogen on the substrate electrode for zinc deposition[19]. The low E_0 values increase the overpotential of hydrogen in the solution and weaken the hydrogen evolution reaction[19,20]. Table 2 shows that the lower E_0 values of solutions B and C than that of solution A indicated that adding Sn or Ga to the base solution can reduce the hydrogen evolution reaction. The lower E_0 value of solution D than those of solutions B and C indicated that the composite additives of Sn and Ga could inhibit the hydrogen evolution reaction more than a single additive. The lower E_0 value of solution F than those of solutions D and E indicated that hydrogen evolution was further inhibited with the increase in Pb of Sn and Ga composite additives.

I_0 is the index of zinc deposition dissolution. High I_0 values accelerate the dissolution rate of zinc deposition[19]. The slightly higher I_0 of solution D than that of solutions B and C indicated that the addition of Sn and Ga in the base solution could obtain higher zinc deposition dissolution rates than a single additive. The slightly lower I_0 values of solutions F and E than that of solution D demonstrated that the increase in Pb reduced the dissolution rate of zinc deposition. The relatively close B_a and B_c of solutions B, C, and D exhibited that the reaction was controlled by the mixture of anode and cathode. However, the larger Tafel slope of solutions A, E, and F than that of the cathode indicated that the reaction was controlled by the anode.

3.3 Analysis of constant-current charge/discharge curve

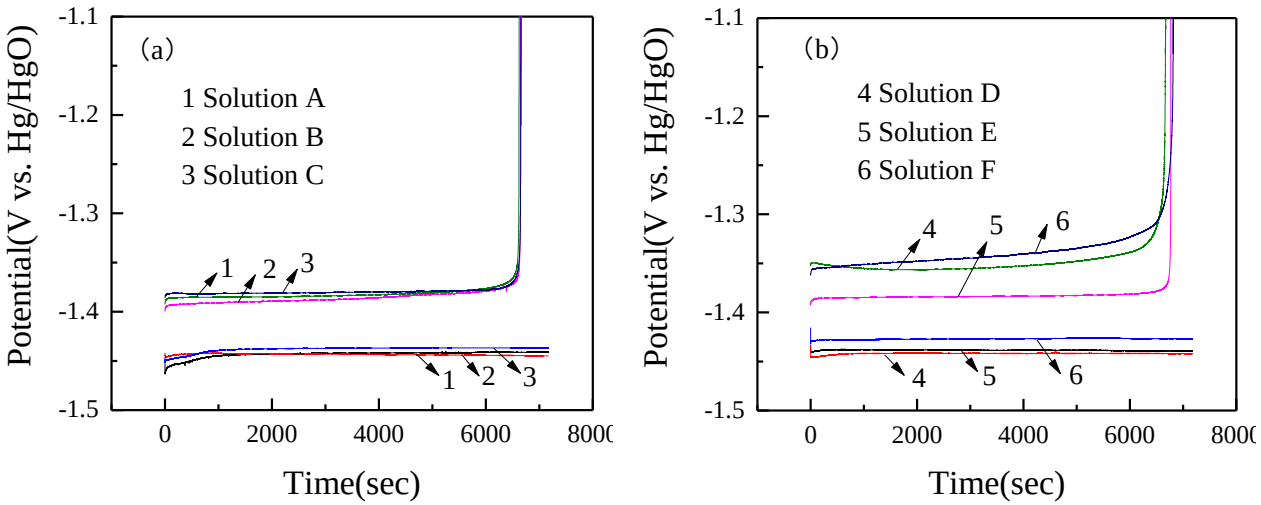

Figure 3. Constant-current charge/discharge curve of the electrode in different solutions (40 mA/cm^2): (a)solutions A, B, and C; (b)solutions D, E, and F

Figure 3 illustrates the charge/discharge curve of the sixth cycle in different solutions charging at a current density of 40 mA/cm^2 for 7200 s and discharge at the same current density to −0.6 V. Figure 3 shows that the voltage of different solutions suddenly decreased to approximately −1.45 V in the initial stage of charging due to the formation of zinc deposition crystal nuclei[13]. The decrease in maximum initial voltage of the base solution indicated that the nucleation needed strong polarization. Compared with the base solution, the smaller initial voltage decrease in the solution with additives and flatter voltage platform indicated that the additives easily produced uniform crystal nuclei and dense deposition layers. The difference between the charging voltage of the basic solution and that of only adding Sn or Ga was insignificant. The addition of Sn and Ga and composite additives significantly increased the charging voltage, and the increase in charging voltage with the increase in Pb concentration indicated that the required charging voltage for the overall battery slightly decreased. The different solutions passed through a stable discharge platform and then increased to the cutoff voltage upon discharge. Coulombic efficiency refers to the ratio of discharge capacity to the charging capacity of the battery. This value evaluates the performance of zinc–nickel single-flow batteries. The coulombic efficiency reached 92% when the basic solution was used in the zinc–nickel single-flow battery. The coulombic efficiency of the additive was slightly higher than that of the basic solution, and solution F obtained the largest value at 94.9%. Compared with the base solution, the discharge voltage was slightly higher when the additives were used, but their overall voltage efficiency was similar. Additives generally improve the coulombic efficiency of zinc–nickel single-flow batteries although the effect remains unclear.

3.4 Analysis of SEM images

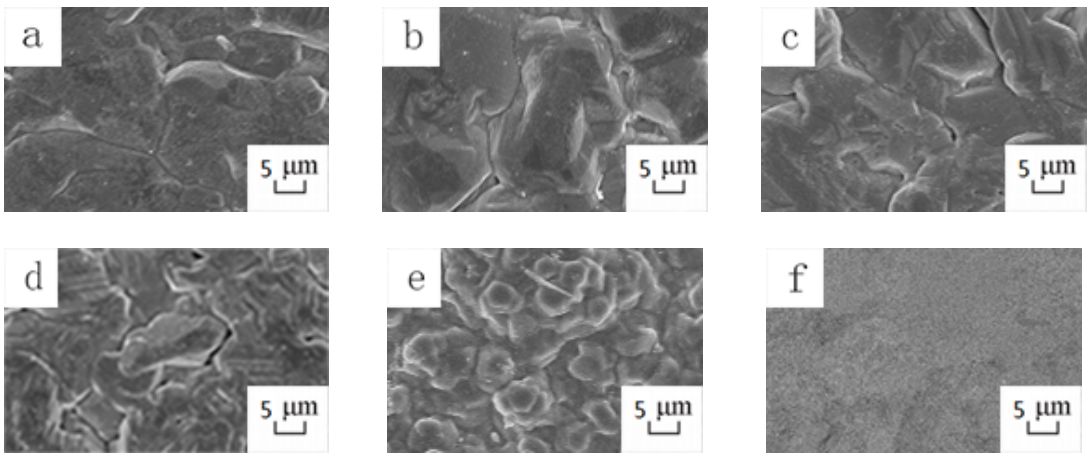

Figure 4. SEM images of the electrode surface in different solutions charging at a current density of 20 mA/cm^2 for 500 s: (a)solutions A; (b)solutions B;(c)solutions C;(d)solutions D;(e)solutions E; (f)solutions F

To further understand the effect of composite additives, the three-electrode system was used to charge and discharge 20 cycles under the condition of a constant current density of 20 mA/cm^2 and then charging for 500 s under the same current density. The coating on the negative electrode surface was compared and analyzed via SEM. The SEM images of the sample surface are shown in Figure 4.

The SEM images illustrated that the electrodeposition of solutions A, B, C, D, and E presented densely layered step particles with unclear dendrites. This finding indicated that the deposition overpotential was high under the experimental conditions in this study, the crystal nucleus on the surface was fully formed, and the macrostep (layered growth) was formed by electrodeposition[21]. When solution F was charged for 500 s at a current density of 20 mA/cm^2, the electrodeposition appeared to be spongy crystal-like structures with small particles and clusters. The size of zinc deposition crystal particles was relatively large in the base solution. Adding Sn or Ga to the base solution can refine the size of zinc deposition particles. When Sn and Ga composite additives were added to the base solution, the size of zinc deposition particles can be further refined (see Figure 4(d)). Compared with the particles shown in Figure 4(d), the zinc deposition particles in Figure 4(e) were clearly smaller and the deposition surface was flatter. This finding demonstrated that the addition of Pb significantly improved the coating morphology during the electrodeposition process. The behavior shown in Figure 4(f) indicated the occurrence of mixed spongy and compact zinc growth due to the increase in Pb concentration[17]. The SEM results were consistent with those of cyclic voltammetry. If the lead ion concentration is increased further, then the spongy zinc deposits will form again[17].

3.5 Analysis of self-discharge

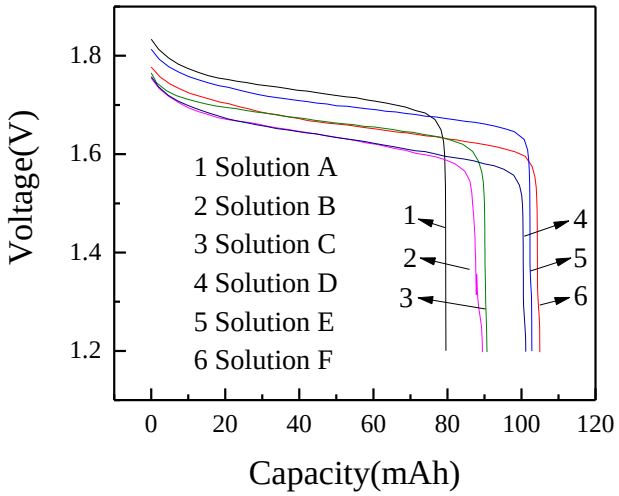

Figure 5. Self-discharge curve of the electrode in different solutions after 24 h of standing

Figure 5 illustrates the self-discharge test chart of different solutions. The battery was charged to 160 mA·h with a constant current of 20 mA/cm^2 current density and allowed to stand for 24 h. During the standing process, the continuously flowing solution was discharged to 1.2 V at a current

density of 20 mA/cm^2[13]. The coulombic efficiency of the base solution was only 49.7% after 24 h in standby state. After adding 0.05 mol/L Sn, 0.05 mol/L Ga, 0.05 mol/L Sn+0.05 mol/L Ga, 0.05 mol/L Sn+0.05 mol/L Ga+0.0001 mol/L Pb, and 0.05 mol/L Sn+0.05 mol/L Ga+0.001 mol/L Pb, the coulombic efficiency was 56%, 56.7%, 63.2%, 64.2%, and 65.6%, respectively. The self-discharge of the base solution was increasingly serious after 24 h in standby state. Self-discharge was inhibited after adding Sn or Ga. The effect of Sn and Ga composite additives was better than that of a single additive. The improvement in self-discharge after adding Pb was unclear.

4. CONCLUSIONS

In this study, the effect of composite additives on the deposition and dissolution of zinc anode for zinc–nickel single-flow batteries was investigated. The following conclusions can be drawn from this study:

1.The negative scanning of cyclic voltammetry curves of the electrode in the solutions with composite additives deviated from the zero line earlier than that in the base solution. The strong cathodic polarization of the electrode in the solutions with the composite additives obtained low deposition potential values. The Tafel polarization curves demonstrated the low E_0 values of the electrode in the solutions with composite additives and the weakened hydrogen evolution reaction.

2. In the constant-current charge/discharge process, compared with the basic solution and a single additive conditions, the composite additives could improve the charge and discharge voltages and increase the coulombic efficiency of composite additives although the improvement was unclear.

3. The SEM results showed that the composite additives significantly improved the morphology of the electrodeposited coating, produced small grains, and increased the crystal growth density. The results of self-discharge showed that Sn and Ga composite additives improved the self-discharge inhibition than that of a single additive and the addition of Pb had a certain degree of improvement on self-discharge inhibition although its concentration must be controlled.

ACKNOWLEDGEMENTS
The authors acknowledge the financial support from the National Natural Science Foundation of China (No. 51776092).

References

1. C.-W. Lee, K. Sathiyanarayanan, S.-W. Eom,*J. Power Sources*,160(2006)1436.
2. B. Szczesniak, M. Cyrankowska, A. Nowacki, *J. Power Sources*, 75(1998)130.
3. F. Li, H.-J Liu, Y.-G. Wang, H.-Q. Li, Y.-Y. Xia, *Chem. J. Chin. Univ*., 28(2007)2133.
4. S.-W. Wang, Z.-H. Yang, L.-H. Zeng, Y.-B. Zhao, X.-W. Wang, *Chin. J. Power Sources*, 32(2008)215.
5. E.-D. Yang, H.-B. Yang, J.-T. Ji, H. Sun, X.-D. Wang, Z.-X. Zhou, H.-T. Yuan, *Chin. J. Power Sources*, 27(2003)31.
6. X.-F. Liu, Y.-G. Tang, Y.-J. Song, W.-Q. Li, *Chin. Battery Ind*., 14(2009)90.

7. K.-L. Liu, P. He, H.-M. Bai, J.-C. Chen, F.-Q. Dong, S.-B. Wang, M.-Q. He, S.-P. Yuan, *Mater. Chem. Phys*., 199(2017)73.
8. J. Cheng, L. Zhang, Y.-S. Yang, Y.-H. Wen, G,-P. Cao, X.-D. Wang, *Electrochem. Commun*., 9(2007)2639.
9. J. Cheng, Y.-H. Wen, G,-P. Cao, Y.-S. Yang,*J. Power Sources*, 196(2011)1589.
10. Y. Ito, M. Nyce, R. Plivelich, M. Klein, D. Steingart, S. Banerjee, *J. Power Sources*, 196(2011)2340.
11. Y.-H, Wen, J. Cheng, L. Zhang, X. Yan, Y.-S. Yang,*J. Power Sources*, 193(2009)890.
12. J.-M. Wang, L. Zhang, C. Zhang, Q. Xiao, J.-Q. Zhang, C.-N. Cao, *J. Funct. Mater*., 32(2001)45.
13. S.-G. Yao, Y. Chen, J. Cheng, Y.-J. Shen, D.-P. Ding, Y.-S. Yang,*Chem. J. Chin. Univ*., 40(2019)481.
14. J. Cheng, Y.-H. Wen, Y. Xu, G,-P. Cao, Y.-S. Yang,*Chem. J. Chin. Univ*., 32(2011)2640.
15. J.-L. Pan, Y.-H. Wen, J. Cheng, G,-P. Cao, Y.-S. Yang, *Chem. J. Chin. Univ*., 33(2012)531.
16. H.-L. Zeng, Electroplating process manual, China Machine Press(1997), China.
17. Y.-H. Wen, J. Cheng, L. Zhang, X. Yan, Y.-S. Yang,*J. Power Sources*, 193(2009)890.
18. Q.-B. Zhang, Y.-X. Hua, *Hydrometallurgy*, 99(2009)249.
19. J.-L. Pan, Y.-H. Wen, J. Cheng, J.-Q. Pan, S.-L. Bai, Y.-S. Yang, *Chin. J. Chem. Eng*., 24(2016)529.
20. L. Zhang, J. Cheng, Y.-S. Yang, Y.-H. Wen, X.-D. Wang, G.-P. Cao, *J. Power Sources*, 179(2008)381.
21. J.-O. Bockris, Z. Nagy, D. Drazic, *J. Electrochem. Soc*.,120(1973)30.